Electronic structures of finite carbon nanotubes under external fields

2006 J. Phys.: Condens. Matter 18 9427

(http://iopscience.iop.org/0953-8984/18/41/009)

INSTITUTE OF PHYSICS PUBLISHING JOURNAL OF PHYSICS: CONDENSED MATTER

J. Phys.: Condens. Matter **18** (2006) 9427–9434 doi:10.1088/0953-8984/18/41/009

Electronic structures of finite carbon nanotubes under external fields

C H Lee[1], R B Chen[2], T S Li[3], C P Chang[4] and M F Lin[1]

[1] Department of Physics, National Cheng Kung University, Taiwan, Republic of China
[2] Center for General Education, National Kaohsiung Marine University, Taiwan, Republic of China
[3] Department of Electrical Engineering, Kun Shan University, Taiwan, Republic of China
[4] Center for General Education, Tainan Woman's College of Arts and Technology, Taiwan, Republic of China

E-mail: mflin@mail.ncku.edu.tw

Received 19 July 2006, in final form 12 September 2006
Published 29 September 2006
Online at stacks.iop.org/JPhysCM/18/9427

Abstract

The electronic states of finite carbon nanotubes in the presence of electric and magnetic fields are calculated by the tight-binding model. Electronic properties such as state energy, energy gap, and density of states are mainly determined by the transverse electric field, the magnetic field, the Zeeman splitting, and the nanotube length, as well as the transverse geometric structure. The electric field could induce the destruction of state degeneracy, produce more low-energy states, and lead to significant changes in energy spacing. Complete energy-gap modulations exist during the variation of the electric field. Such effects are enhanced by the magnetic field.

1. Introduction

Carbon nanotubes (CNs) have attracted much attention since they were discovered by Iijima in 1991 [1]. The electronic properties of CNs depend on both their radii and chirality. A single-walled CN is formed by rolling a 2D graphite sheet, and is a member of the quasi-one-dimensional system. A finite CN can be obtained by cutting an infinite long system. It could be regarded as a zero-dimensional quantum dot. The reduction in dimensionality leads to the quantization of electronic states [2, 3]. This phenomenon has been verified by scanning tunnelling microscopy and transport experiments [3–8]. Finite CNs also exhibit many interesting physical properties, e.g., electronic structures [9, 10], magnetic properties [11, 12], and optical excitations [13]. The electronic states have been calculated from the first-principles local-density approximation [2, 9, 10] and the tight-binding model [11–13]. In this work, the electronic structures of finite CNs under external fields are studied with the tight-binding model. The dependence on the transverse geometry, the nanotube length, the magnetic field, and the transverse electric field is investigated in detail.

Knowledge of the CN behaviour in an external electric field is helpful for designing nanoscale devices. Electromechanical systems based on CNs have been constructed experimentally [14]. Electronic devices including single-electron transistors, field-effect transistors, and diodes also have made remarkable advances [15–17]. The applied transverse electric field gives rise to an extra potential on the nanotube surface and changes the physical properties. Its effects on the electronic structures of infinite CNs [18–21] and carbon tori [22] have been studied. The transverse electric field would strongly influence their energy structures and optical properties. Compared with the magnetic field, the availability of electric field-controlled modulations is an advantage in implementing nanoelectronic applications.

There are a lot of theoretical and experimental studies on magnetoelectronic properties of infinite CNs [23–27]. Electronic properties, such as state energy, state degeneracy, and energy gap, could be drastically changed by the magnetic field. The spin-B interaction (Zeeman splitting) could induce a semiconductor–metal transition and play an important role in the magnetoelectronic properties [28, 29]. Furthermore, the magnetoelectronic properties of finite CNs have been investigated theoretically [11, 12]. Due to their distinctive edge or boundary states, the magnetic properties of finite CNs are different from those of infinite CNs. The special magnetic susceptibility and magnetization could be verified in experimental measurements. The coupling of electric and magnetic fields would be expected to alter the localized states and modify the energy gap.

2. Theory

A finite CN could be regarded as a rolled-up graphite sheet and is uniquely characterized by using a lattice vector $\mathbf{R_x} = m\mathbf{a_1} + m\mathbf{a_2}$, where $\mathbf{a_1}$ and $\mathbf{a_2}$ are the primitive lattice vectors of a graphite sheet (for details see [13]). The radius and chiral angle are, respectively, $r = b\sqrt{3(m^2+mn+n^2)}/2\pi$ and $\theta = \tan^{-1}[-\sqrt{3}/(2m+n)]$. $b = 1.42$ Å is the C–C bond length. The length of the tube is determined by the total number of carbon atoms (N_A). $(m, n; N_A)$ is used to represent a finite CN.

The π-electronic states of a finite CN are calculated from the tight-binding model within the nearest-neighbour interactions. When a finite CN is threaded by a uniform magnetic field, the calculations become more complicated. The angle between the magnetic field and the tube axis is assumed to be α, i.e., $\mathbf{B} = B\cos\alpha\hat{z} + B\sin\alpha\hat{r} = B_{\parallel}\hat{z} + B_{\perp}\hat{r}$. It is convenient to using cylindrical coordinates (r, Φ, z), and the vector potential is chosen to be $\mathbf{A} = rB\cos\alpha/2\hat{\Phi} + rB\sin\alpha\sin(x/r)\hat{z}$ $(x = r\Phi)$. The x or Φ dependence means that all carbon atoms N_A need to be included in the Hamiltonian matrix elements. The nearest-neighbour Hamiltonian matrix built from the N_A tight-binding functions is given by

$$H_{ij} = \gamma_{ij} e^{i(\phi\cos\alpha/\phi_0)\Delta x/r} e^{i\frac{e}{\hbar}\Delta G}. \tag{1}$$

$\mathbf{R}^i = (x, z)$, $\mathbf{R}^j = (x', z')$, and $\Delta\mathbf{R} = \mathbf{R}^j - \mathbf{R}^i = (\Delta x, \Delta z)$. $\mathbf{R}^i = (x, z)$ and $\mathbf{R}^j = (x', z')$ are, respectively, positional vectors for the ith atom and the jth atom. $\gamma_{ij} = \gamma_0[1 - (\Delta x)^2/8r^2]$ is the nearest-neighbour hopping integral [13, 30], and γ_0 is that of a graphite sheet. γ_{ij} is mainly determined by the curvature effect (the misorientation of the $2p_z$ orbitals on the cylindrical surface). The magnetic flux is $\phi = \pi r^2 B$ and $\phi_0 = hc/e$. The vector potential will induce the Peierls phase where the phase difference due to the perpendicular magnetic field ($B\sin\alpha\hat{r}$) is

$$\begin{aligned} \Delta G &= \frac{\phi\Delta z\sin\alpha}{\pi\Delta x}\left[\cos\frac{x}{r} - \cos\frac{x+\Delta x}{r}\right], \qquad \Delta x \neq 0, \\ &= \frac{\phi\Delta z\sin\alpha}{\pi r}\sin\frac{x}{r}, \qquad \Delta x = 0. \end{aligned} \tag{2}$$

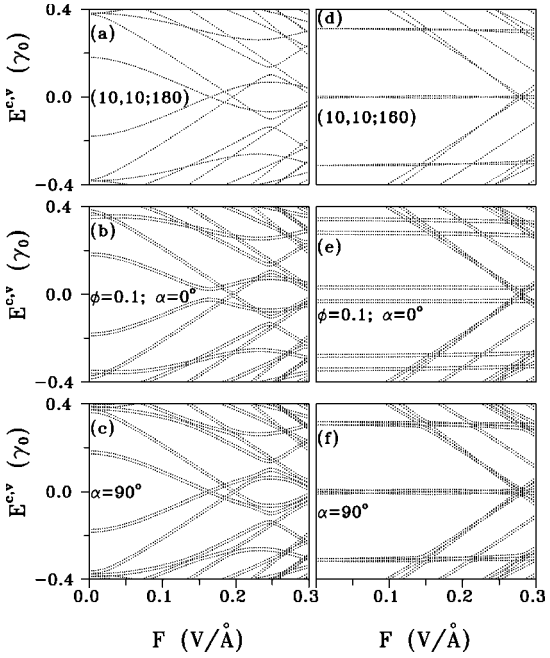

Figure 1. The energy spectra versus the traverse electric field for the (10, 10; 180) carbon nanotube at (a) $\phi = 0$, (b) $\phi = 0.1\phi_0$ and $\alpha = 0°$; (c) $\phi = 0.1\phi_0$ and $\alpha = 90°$. The same plots for the (10, 10; 160) carbon nanotube are, respectively, shown in (d), (e); (f). The Zeeman splitting is taken into account.

When a finite CN exists in a transverse electric field F, the on-site energies of carbon atoms are changed and the diagonal Hamiltonian matrix element is expressed as

$$H_{ii} = -eV\cos(\Phi_i), \tag{3}$$

where $V = rF$ is the electric potential from the effective electric field and Φ_i is the azimuth angle of the ith atom.

By diagonalizing the Hamiltonian matrix, the state energy $E^{c,v}(F,\phi)$ and wavefunction $\Psi^{c,v}(F,\phi)$ can be obtained. The magnetostate energy $E^{c,v}(F,\phi,\sigma)$ is the sum of the state energy plus the Zeeman energy when the spin-B interaction is considered. The value of the Zeeman energy $E(\sigma,\phi)$ is $g\sigma\phi/m^*r^2\phi_0$. The g factor is assumed to be the same as that ($\sim$2) of graphite, and $\sigma = \pm 1/2$ is the electron spin. The spin-B interaction causes separation of the spin-up and spin-down states and the feature can be observed in the density of states (DOS). The DOS of a finite CN is defined as

$$D(\omega, F, \phi) = \sum_{h=c,v} \frac{1}{\pi} \frac{\Gamma}{[\omega - E^h(F,\phi,\sigma)]^2 + \Gamma^2}, \tag{4}$$

where Γ ($=10^{-4}\gamma_0$) is the broadening energy width.

3. Results and discussion

The low-energy states of the (10, 10; 180) armchair CN with the transverse electric field are shown in figure 1(a). The (10, 10; 180) CN has a moderate energy gap (type-I) and the π-

electronic structure is symmetric about $E_F = 0$. The states near $0.38\gamma_0$ are fourfold degenerate and others are doubly degenerate if the spin degeneracy is taken into account. The energy gap is modulated and the fourfold degeneracy is changed into double degeneracy after applying an electric field F. E_g decreases with increasing F and vanishes at $F \simeq 0.16$ V Å^{-1}. When the magnitude of F continues to grow, there are more low-energy states and a complicated variation of E_g. Furthermore, an additional magnetic field ($\phi = 0.1\phi_0$ and $\alpha = 0°$) is also considered simultaneously (figure 1(b)). The parallel magnetic field affects the state energies and it further destroys the state degeneracy by the spin-B interaction. The state crossing vanishes at $F \simeq 0.16$ V Å^{-1}, and there exists an energy gap. The vanishing E_g happens at the larger electric field $F \simeq 0.2$ V Å^{-1}. When the magnetic field is perpendicular to the nanotube axis, the change of state energies with the electric field is similar to that in figure 1(a) except for the Zeeman splitting, as shown in figure 1(c). For the (10, 10; 160) CN, an armchair CN with another length, a narrow energy gap (type-II) exists at zero external fields (figure 1(d)). The energy gap is weakly affected by the electric field, while it becomes vanishing at certain values of F. The electronic states nearest to the Fermi level, which determine the energy gap, are localized at different armchair lines without any hoppings. The effect on band structures combined with the parallel magnetic field is distinct from that in figure 1(b). The parallel magnetic field has a strong effect on the energy gap (figure 1(e)). At small F, $B_\parallel$ hardly affects the dependence of E_g on the electric field, or the localization of the lowest electronic states. The state degeneracy and its dependence on external fields are similar for both the (10, 10; 160) and (10, 10; 180) CNs. That is to say, the electric and magnetic fields, respectively, destroy the fourfold degeneracy (figures 1(d) and (a)) and the double degeneracy (figures 1(e) and (b)). After changing the angle α from 0° to 90°, the condition is identical to that of the above-mentioned (10, 10; 180) CN.

The finite zigzag CN under external fields is more interesting because of the localized edge states induced by its transverse zigzag structure. The edge states with zero energy (type-III) come from the $2p_z$ orbitals localized at the outermost zigzag positions, and they are fourfold degenerate. In figure 2(a), the localized states do not open an energy gap with increasing F even if F reaches 0.3 V Å^{-1}. But an energy gap is opened and the fourfold degeneracy is thoroughly broken when $B_\parallel$ and F are applied simultaneously, as presented in figure 2(b). Such an effect does not occur with the coupling of the transverse magnetic and electric fields (figure 2(c)). Moreover, an energy gap is opened, only owing to the Zeeman splitting. Finally, a finite chiral (12, 6; 180) CN is considered and compared with the foregoing finite CNs (figures 2(d)–(f)). A (12, 6; 180) CN also has a moderate gap so its variation under external fields should be similar to that of the (10, 10; 180) CN. In brief, finite CNs can be classified into three categories according to their energy gaps, and they have different responses to the electric field.

The low-energy DOSs of the (10, 10; 180) CN under external fields are shown in figure 3(a). For discrete states, the DOS would be delta-function-like, and the heights of peaks are related to the state degeneracy. There are two doubly degenerate peaks and one fourfold degenerate peak at $\omega < 0.4\gamma_0$ with zero external field (the solid curve). The electric field lifts the fourfold degeneracy and changes the frequencies of the peaks. Moreover, the double degeneracy is further broken by the spin-B interaction. The differences in DOS between $B_\parallel$ and $B_\perp$ are relatively obvious at the high-frequency range ($\omega > 0.35\gamma_0$). Under the external fields, the DOS of another length armchair (10, 10; 160) CN exhibits similar behaviour, as shown in figure 3(b). The fourfold and double degeneracy are broken, respectively, by the electric and magnetic fields. The electric field F has a weak effect on the peak frequencies of the (10, 10; 160) CN. For the narrow-gap (10, 10; 160) CN, the parallel magnetic field is more efficient in modulating the peak frequencies than the transverse magnetic fields, and its

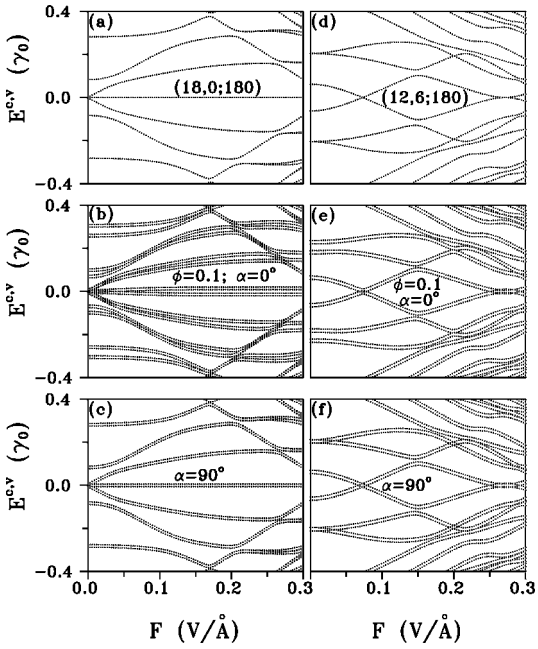

Figure 2. Similar plots as figure 1, but calculated for the (18, 0, 180) carbon nanotube in (a)–(c) and the (12, 6; 180) carbon nanotube in (d)–(f).

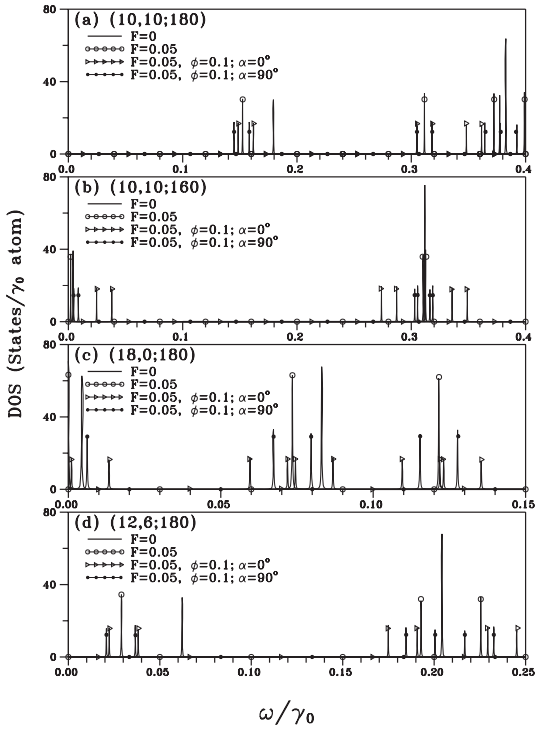

Figure 3. Density of states of the (a) (10, 10; 180), (b) (10, 10; 160), (c) (18, 0; 180), and (d) (12, 6; 180) carbon nanotubes at $F = 0.05$ and $\phi = 0.1\phi_0$ with different α's.

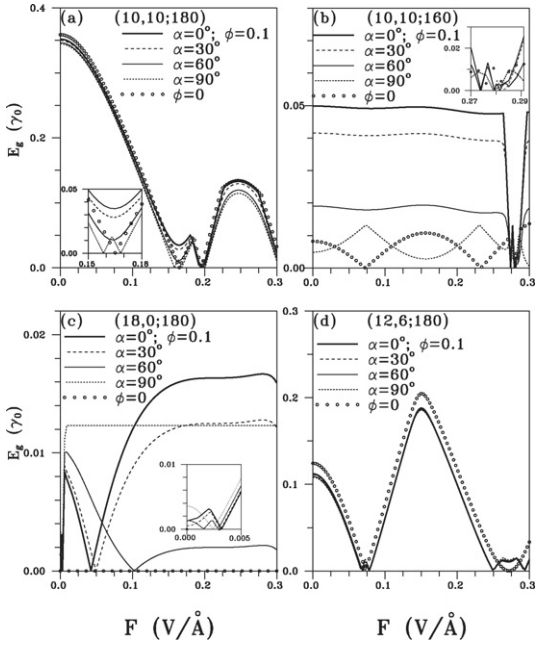

Figure 4. The electric-field-dependent band gap for the (a) (10, 10; 180), (b) (10, 10; 160), (c) (18, 0; 180), and (d) (12, 6; 180) carbon nanotubes at $\phi = 0.1$ and different values of α. The result at $\phi = 0$ is also calculated for comparison. The insets in (a)–(c) show the details near complete energy-gap modulations.

effect is even more significant than that of the electric field. The edge states of the (18, 0; 180) CN play an important role in the DOS. In figure 3(c), all the low-energy states of the (18, 0; 180) CN are fourfold degenerate. After F is applied, the peak frequencies and the energy spacing between two neighbouring peaks are modulated. But their heights remain unchanged at $F = 0.05$ V Å^{-1}. The edge states with zero energy, as discussed earlier, are scarcely influenced by the electric field or the magnetic field [11, 12]. For F and $B_{\parallel}$, the edge states become separated and each peak resolves into four lowest peaks. As to F and $B_{\perp}$, the fourfold degenerate peak just becomes two doubly degenerate peaks because of the Zeeman splitting. For the (12, 6; 180) CN, the above-mentioned effects that are induced by the combination of the electric and magnetic fields could be verified (figure 3(d)).

In figure 4(a), the variations of E_g for the type-I (10, 10; 180) CN with $\phi = 0.1$ and different values of α are presented. E_g oscillates significantly with increasing F. There exist complete energy-gap modulations ($E_g = 0 \leftrightarrow E_g \neq 0$) at 0.15 V Å^{-1} $< F <$ 0.2 V Å^{-1}. Such modulations happen more frequently when the magnetic field is perpendicular to the nanotube axis (see the inset). For the chiral (12, 6; 180) CN, the variation of E_g would be analogous to that of the type-I (10, 10; 180) CN (figure 4(d)). The energy gap is also strongly affected by the length of the CN, as shown in figure 4(b). For the type-II (10, 10; 160) CN, E_g increases and reveals a flat structure after the $\alpha \neq 90°$ magnetic field is applied. But an oscillatory feature also occurs at $\alpha = 90°$ and $\phi = 0$. The electric field could induce complete energy-gap modulations alone, as seen in type-I CNs. At large F, the sharp variation of the energy gap or the complete energy-gap modulation derives from more low-energy states caused by the electric field (figure 1(e)). The type-III (18, 0; 180) CN holds the localized state and does

not cause an energy gap with growing F (open circles in figure 4(c)). The Zeeman splitting would open an energy gap at $F = 0$ (inset in figure 4(c)). A rapid variation arises at small F because the energy spacing could be modulated by the electric field. There are different causes of energy gap production with the inclusion of magnetic field. For $\alpha \neq 90°$, E_g would originate from the separation of the localized edge states, whereas E_g would only originate from the Zeeman splitting for $\alpha = 90°$. So the $\alpha \neq 90°$ magnetic field could induce complete energy-gap modulation at the moderate F.

4. Conclusions

In conclusion, the electronic properties of finite CNs rely sensitively on the nanotube geometry (the length and the transverse geometric structure), the transverse electric field, the magnetic field, and the Zeeman effect. The electric field would break the state degeneracy, vary the energy spacing, and increase the number of low-energy states. Such effects could be enhanced by an additional magnetic field. The coupling of the electric and parallel magnetic fields could separate the localized states and modulate the energy gap. The influence of the transverse magnetic field on the electronic structures originates from the Zeeman splitting. Type-I, type-II, and type-III finite CNs could exhibit complete energy-gap modulations via the coupling of electric and magnetic fields.

Acknowledgment

This work is supported in part by the National Science Council of Taiwan under Grant No. NSC 94-2112-M-006-002.

References

[1] Iijima S 1991 *Nature* **354** 56
[2] Rubio A, Sánchez-Portal D, Artacho E, Ordejáin P and Soler J M 1999 *Phys. Rev. Lett.* **82** 3520
[3] Venema L C, Wildöer J W G, Janssen J W, Tans S J, Hinne L J, Tuinstra T, Kouwenhoven L P and Dekker C 1999 *Science* **283** 52
[4] Tans S J, Devoret M H, Groeneveld R J A and Dekker C 1998 *Nature* **394** 761
[5] Nygård J, Cobden D H and Lindelof P E 2000 *Nature* **408** 342
[6] Cobden D H and Nygård J 2002 *Phys. Rev. Lett.* **89** 046803
[7] Jarillo-Herrero P, Sapmaz S, Dekker C, Kouwenhoven L P and Van der Zant H S J 2004 *Nature* **429** 389
[8] Moriyama S, Fuse T, Suzuki M, Aoyagi Y and Ishibashi K 2005 *Phys. Rev. Lett.* **94** 186806
[9] Jishi R A, Bragin J and Lou L 1999 *Phys. Rev.* B **59** 9862
[10] Matsuo Y, Tahara K and Nakamura E 2003 *Org. Lett.* **5** 3181
[11] Chen R B, Lu B J, Tsai C C, Chang C P, Shyu F L and Lin M F 2004 *Carbon* **42** 2873
[12] Chen R B, Chang C P, Hwang J S, Chuu D S and Lin M F 2005 *J. Phys. Soc. Japan* **74** 1404
[13] Chen R B, Chang C P, Shyu F L, Hwang J S and Lin M F 2004 *Carbon* **42** 531
[14] Kim P and Lieber C M 1999 *Science* **286** 2148
[15] Tans S J, Devoret M H, Dai H, Thess A, Smalley R E, Geerligs L J and Dekker C 1997 *Nature* **386** 474
[16] Tans S J, Verschueren A R M and Dekker C 1998 *Nature* **393** 49
[17] Yao Z, Postma H W Ch, Balents L and Dekker C 1999 *Nature* **402** 273
[18] Zhou X, Chen H and Zhong-can O Y 2001 *J. Phys.: Condens. Matter* **13** L635
[19] Li Y, Rotkin S V and Ravailoli U 2003 *Nano Lett.* **3** 183
[20] Pacheco M, Barticevic Z, Rocha C G and Latgé A 2005 *J. Phys.: Condens. Matter* **17** 5839
[21] Li T S and Lin M F 2006 *Phys. Rev.* B **73** 075432
[22] Rocha C G, Pacheco M, Barticevic Z and Latgé A 2004 *Phys. Rev.* B **70** 233402
[23] Ajiki H and Ando T 1993 *J. Phys. Soc. Japan* **62** 1255
[24] Ajiki H and Ando T 1993 *J. Phys. Soc. Japan* **62** 2470

[25] Ajiki H and Ando T 1995 *J. Phys. Soc. Japan* **64** 4382
[26] Lin M F and Shung K W K 1995 *Phys. Rev.* B **52** 8423
[27] Shyu F L, Chang C P, Chen R B, Chiu C W and Lin M F 2003 *Phys. Rev.* B **67** 045405
[28] Chiu C W, Shyu F L, Chang C P, Chen R B and Lin M F 2003 *Phys. Lett.* A **311** 53
[29] Chiu C W, Chang C P, Shyu F L, Chen R B and Lin M F 2003 *Phys. Rev.* B **67** 165421
[30] Kane C L and Mele E J 1997 *Phys. Rev. Lett.* **78** 1932